Available online at www.sciencedirect.com

SciVerse ScienceDirect

Ceramics International 39 (2013) 3043–3048

CERAMICS INTERNATIONAL

www.elsevier.com/locate/ceramint

Growth of ZnO hemispheres on silicon by a hydrothermal method

Young-Seok Lee[a], Sung-Nam Lee[b,*], Il-Kyu Park[a,*]

[a]Department of Electronic Engineering, Yeungnam University, Gyeongbuk 712-749, South Korea
[b]Department of Nano-Optical Engineering, Korea Polytechnic University, Siheung 429-793, South Korea

Received 22 August 2012; received in revised form 24 September 2012; accepted 25 September 2012
Available online 6 October 2012

Abstract

This paper reports a hydrothermal method to control the morphology of hemisphere ZnO nanostructures (NSs) fabricated on a Si substrate by using surfactant additive molecules. The shape of ZnO NSs was controlled by the concentration of the trisodium citrate (TSC) added during the main growth step. With increasing the TSC concentration from 0 to 1.3 and 2.6 mM, the shape of ZnO NSs changed from a bundle of nanorods to a flower-like-shape composed of merged large hexagonal crystals, and finally to ZnO hemispheres. X-ray diffraction and photoluminescence spectroscopy revealed that the ZnO NSs had a wurtzite crystalline structure. The shape evolution mechanism of ZnO NSs could be explained using the surfactant-mediated growth model.

Keywords: D. ZnO; Hemisphere; Hydrothermal method; Surfactant

1. Introduction

Low-dimensional zinc oxide (ZnO) nanostructures (NSs) have attracted considerable attention due to their direct wide band gap of 3.37 eV, large exciton binding energy of 60 meV and large piezoelectric coefficient [1–3]. These properties have prompted interest in ZnO NSs for electronic, piezoelectric, thermoelectric, electrochemical and optoelectronic applications [1–3]. Preferred directional growth along the *c*-direction of the wurtzite crystal structure makes one-dimensional ZnO NSs promising building blocks for a range of novel nano-device applications [2,3]. Furthermore, ZnO NSs of various shapes can enhance device performance by being integrated into light-emitting devices [4–6], photovoltaic devices [7], or chemical sensors [8]. In particular, hemispherical ZnO NSs are effective for enhancing the performance of optoelectronic devices [4–7]. Therefore, understanding the mechanism and control of the shape evolution of ZnO NSs is very important for enhancing the device performance. Recently, a few methods have been reported for the fabrication of ZnO hemispheres [7,9] or spheres using a solution growth method [10,11]. However, these methods require complicated nano-patterning processes or result in homogeneously formed ZnO spheres in solution. To increase the compatibility of ZnO NSs with other devices, the fabrication process should be simple without using any complicated patterning process and ZnO NSs should be formed on a range of substrates. This paper reports a simple hydrothermal method to control the morphology and shape evolution mechanism of ZnO NSs without a nano-patterning process on a Si substrate using surfactant additive molecules.

2. Experimental details

2.1. Experimental

The ZnO nanostructures (NSs) with different shapes were fabricated on *n*-Si (100) substrates using a two-step hydrothermal method; involving formation of a ZnO seed and main ZnO NS layers [4,12,13]. The shape of ZnO NSs was controlled based on the molar concentration of charged ionic species (citrate ions) during growth of the ZnO NS layers. The seed layer was formed by dipping the cleaned Si substrate into a mixed solution of 40 mM zinc nitrate hexahydrate [$Zn(NO_3)_2 \cdot 6\,H_2O$, 98%, Sigma-Aldrich] and 40 mM hexamine [$(CH_2)_6N_4$, 99.0%, Sigma-Aldrich] dissolved in ethanol followed by annealing at 100 °C for 3 min to produce the three-dimensional ZnO nanodots. After forming the ZnO seed

*Corresponding authors. Tel.: +82 538 103 093; fax: +82 538 104 770.
E-mail addresses: snlee@kpu.ac.kr (S.-N. Lee), ikpark@ynu.ac.kr (I.-K. Park).

0272-8842/$ - see front matter © 2012 Elsevier Ltd and Techna Group S.r.l. All rights reserved.
http://dx.doi.org/10.1016/j.ceramint.2012.09.083

layers, main growth of the ZnO NSs was performed in a mixed solution of 56 mM zinc acetate dihydrate [$Zn(CH_3COO)_2 \cdot 2H_2O$, 99.999%, Sigma-Aldrich] and 200 mM NH_4OH [25–27.9%(NH_3), Kanto Chemical] dissolved in DI water at 95 °C for 1.5 h. Trisodium citrate [HOC-(COONa)($CH_2COONa)_2$; TSC, 99%, Yakuri chemical] was added at various molar concentrations of 0, 0.65, 1.3, 2.6, and 3.9 mM to control the shape of the ZnO NSs.

2.2. Characterizations

Structural properties of ZnO NSs were investigated by field emission scanning electron microscopy (FE-SEM, Hitachi, S-4800) and X-ray diffraction (XRD, PANalytical, MPD for thin film) with an excitation source of Cu Kα radiation. The chemical composition of deposited ZnO NSs was measured by using an energy dispersive X-ray spectroscopy (EDS, Hitachi, S-4800) attached to the FE-SEM. Optical properties of ZnO NSs were examined by photoluminescence (PL) spectroscopy using a 24 mW power 325 nm continuous He–Cd laser (Kimmon Koha) at room temperature. The laser was focused onto the sample surface by an objective lens; the excitation area was estimated to be approximately 400 μm in diameter.

3. Results and discussion

Fig. 1(a) and (b) shows FE-SEM images of the ZnO seed layers before growth of the main ZnO NS layers. The spherical-shaped ZnO nanodots were formed on the Si substrate during seed layer growth in order to minimize the total surface free energy. The mean diameter and density of the ZnO nanodots were 86 nm and $4.42 \times 10^8\ cm^{-2}$, respectively. Fig. 1(c) and (d) shows the ZnO NSs formed after main growth without addition of TSC surfactant. The ZnO NSs were flower-shaped and composed of a bundle of narrow ZnO nanorods with other branches grown from the center junctions as noted arrow in Fig. 1(d). The density of the ZnO NSs was $2.74 \times 10^8\ cm^{-2}$, which was lower than that of the ZnO seed layers. The lower density of ZnO NSs compared to that of the seeds could be attributed to melting of the smaller ZnO nanodots in the main growth solution containing OH^- ions from NH_4OH. Flower-shaped ZnO initial layers are necessary for the formation of hemispherical ZnO NSs, which are thermodynamically unstable due to high surface energy.

Fig. 2(a)–(j) shows FE-SEM images of ZnO NSs grown on Si substrates at different TSC concentrations from 0 to 3.9 mM during the main growth step. As discussed above, ZnO nanorod bundles were formed without addition of TSC. With increasing the TSC concentration from 0 to 1.3 and 2.6 mM, the bundle of ZnO nanorods consisting of flower-shaped ZnO NSs merged together to form large hexagonal crystals, and the morphology of ZnO NSs on the Si substrate changed to a hemispheric shape. The ZnO NSs began to disappear as the TSC concentration was further increased to 3.9 mM. This shape transition mechanism of ZnO NSs on Si substrate is discussed later in the context of surfactant-mediated growth by presenting the schematics. Fig. 3(b) and (d) shows the EDS results of ZnO NSs grown both with and without the addition of 2.6 mM TSC. The EDS spectra of both types of ZnO NSs showed only Zn, O and Si peaks without additional elemental peaks. This suggests that no additional elements were incorporated into the ZnO NSs when TSC was added to the main growth solution. Therefore, ZnO NSs grown on Si substrate can be controlled from a bundle of nanorods to a hemispherical shape by varying the molar content of TSC.

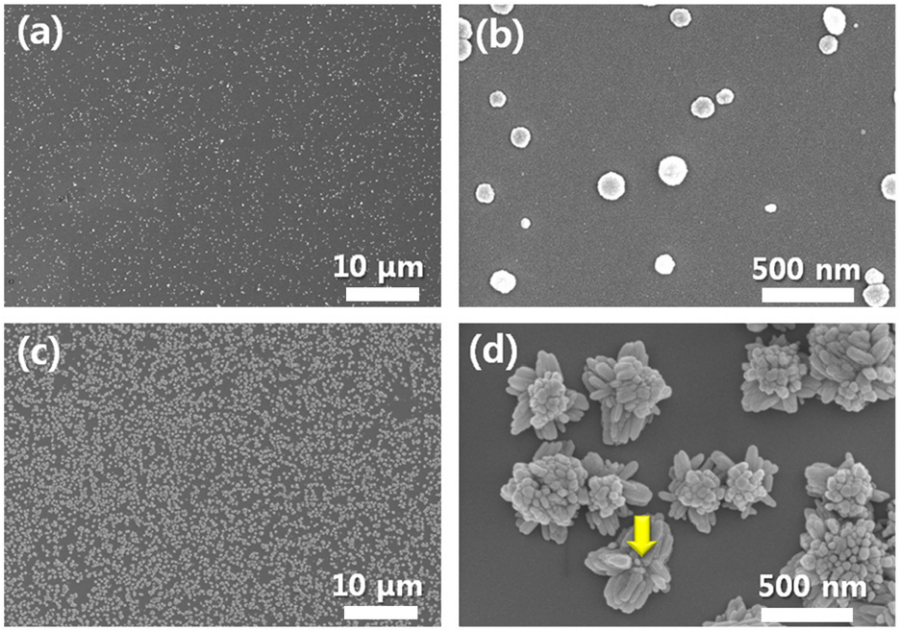

Fig. 1. FE-SEM images of (a) and (b) the ZnO seed, (c) and (d) ZnO NS layers grown on *n*-Si (100) substrates without adding TSC. The arrow in the figure indicates the center junction as discussed in the manuscript.

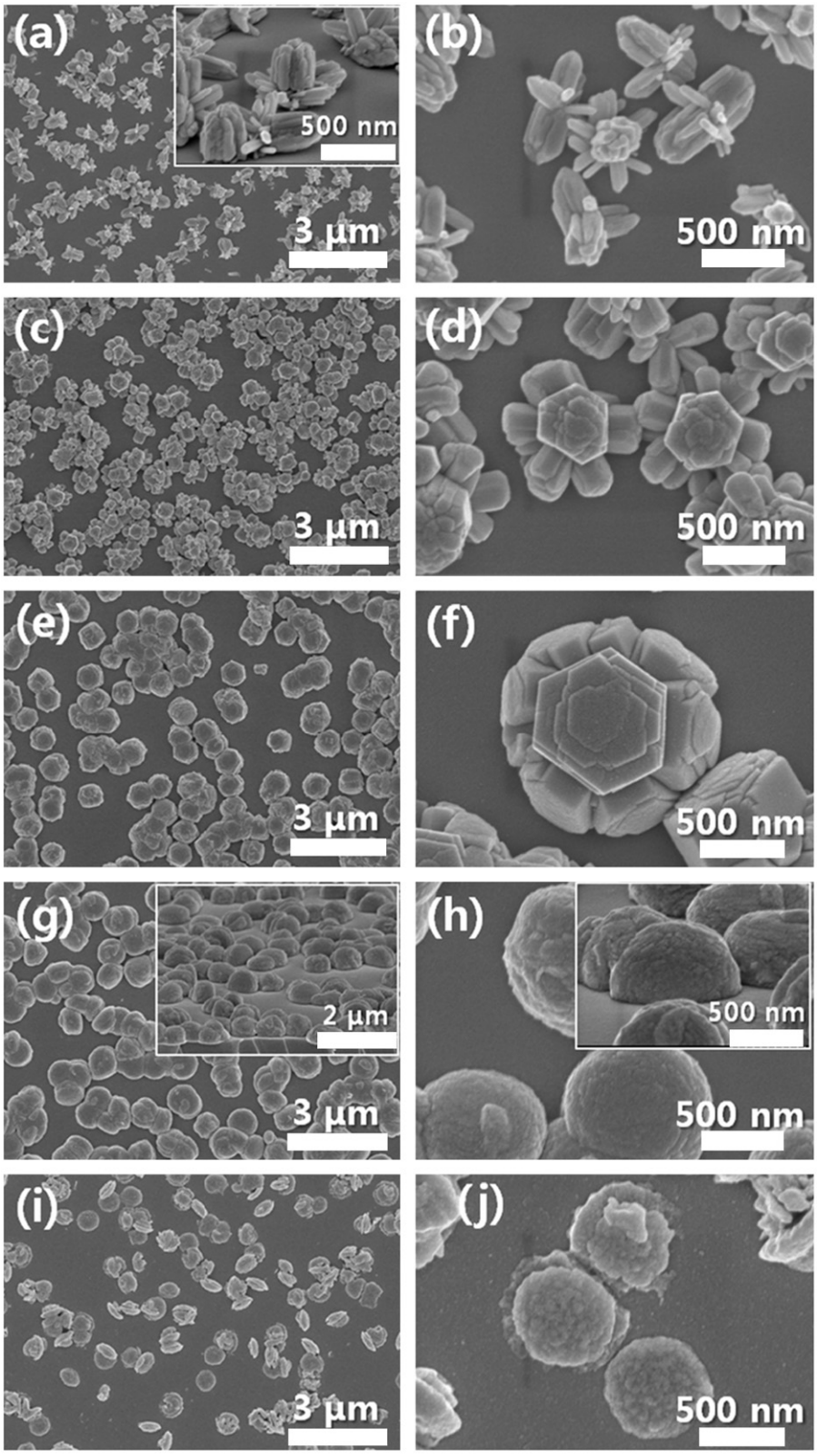

Fig. 2. FE-SEM images of the ZnO NSs grown on *n*-Si (100) substrates with the TSC concentration of (a) and (b); 0 mM, (c) and (d); 0.65 mM, (e) and (f); 1.3 mM, (g) and (h); 2.6 mM, and (i) and (j); 3.9 mM in the main solution.

Fig. 4(a) shows the XRD patterns of ZnO NSs grown on Si substrates at different TSC concentrations ranging from 0 to 3.9 mM during the main growth step. The XRD patterns of all samples showed characteristic wurtzite patterns (JCPDS no. 36-1451) without other peaks. This suggests that all ZnO NSs had a wurtzite crystal structure,

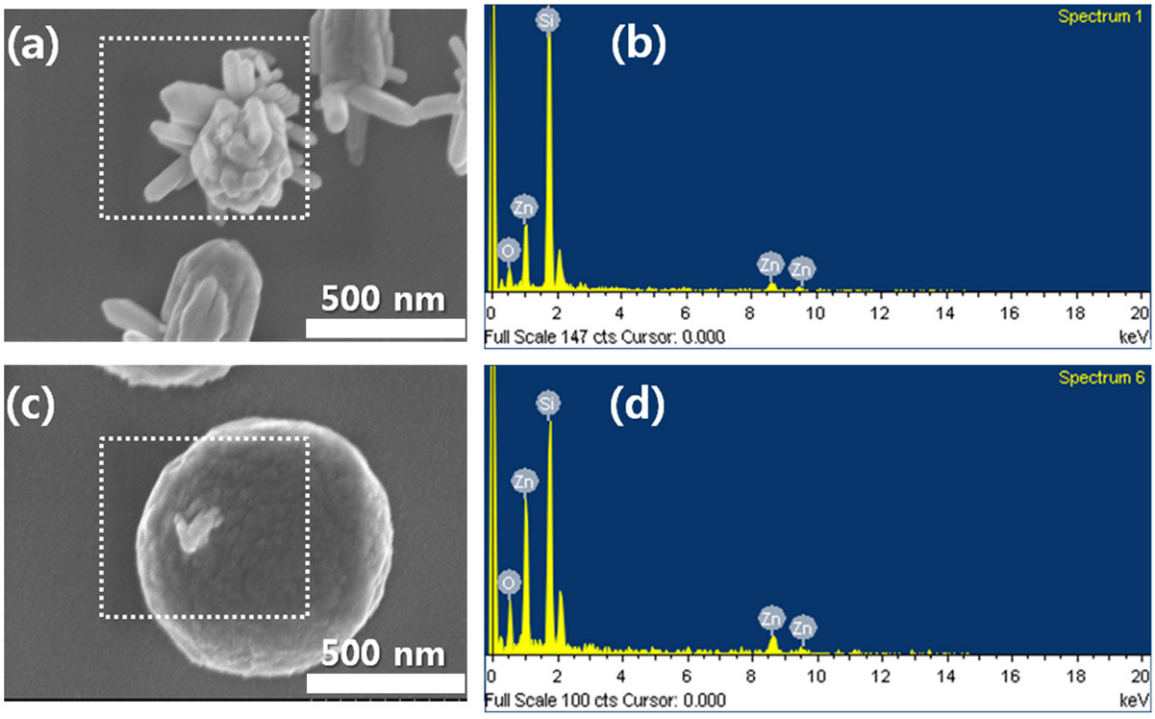

Fig. 3. Enlarged images and EDS patterns of ZnO NSs with the TSC concentration of (a) and (b); 0 mM, and (c) and (d); 2.6 mM in the main solution.

even though the morphology differed according to the TSC concentration. To investigate the effect of TSC addition on the structural properties of ZnO NSs, the integrated intensity and full-width at half-maximum (FWHM) of the (002) peak was plotted as a function of the TSC concentration, as shown in Fig. 4(b). The integrated (002) peak intensity increased linearly with increasing TSC concentration up to 1.3 mM and then decreased with further increases in TSC concentration. The FWHM of the (002) peak showed a low value for the ZnO NSs at a TSC concentration between 1.3 and 2.6 mM. The integrated (002) peak intensity reflects the area fraction of the *c*-plane of the ZnO NSs. Therefore, the increase in integrated (002) peak intensity with increasing TSC molar content up to 1.3 mM could be attributed to an increase in the area of the ZnO *c*-planes, as shown in Fig. 2. With increasing TSC molar content to higher than 1.3 mM, the peak intensity decreased due to reduction in the c-plane of the ZnO NSs. XRD confirmed that the crystal structure of the ZnO NSs remained a wurtzite structure as the area fraction of the (0001) plane varied.

Based on these structural investigations, Fig. 5 presents a schematic diagram of the shape evolution of ZnO NSs according to TSC concentration during the main growth step. In detail, bundles of ZnO nanorods are formed in the absence of TSC. The polar (0001) plane of the ZnO has a relatively higher surface energy than the six nonpolar $\{10\bar{1}0\}$ planes. Therefore, ZnO grows preferentially along the [0001] direction to form a nanorod bundle by minimizing the exposed (0001) planes. The reaction involved in the formation of ZnO NSs in aqueous ammonia solution can be expressed as follows:

$$Zn(CH_3COO)_2 \cdot 2H_2O \rightarrow Zn^{2+} + 2CH_3COO^- + 2H_2O$$

$$NH_4OH \rightarrow NH_3 + H_2O \rightarrow NH^{4+} + OH^-$$

$$Zn^{2+} + NH_3 \rightarrow Zn(NH_3)_4^{2+}$$

$$Zn(NH_3)_4^{2+} + OH^- \rightarrow ZnO$$

The growth kinetics of a ZnO crystal depends on the formation of hydroxide ions (OH^-) and $Zn(NH_3)_4^{2+}$. A large amount of these ions produced by hydration of aqueous ammonia during the initial stage causes rapid growth resulting in the formation of twin boundaries that act as a center junction for the ZnO branches, as mentioned above [10]. When a small amount of TSC is added, the bundle of ZnO nanorods merge together to form large hexagonal crystals. TSC is an effective suppressor of ZnO [0001] directional growth [10,11] and generates bulky citrate ions when dissolved in aqueous solution according to following reaction [10]:

$$[C_6H_5O_7]^{3-} + H_2O \leftrightarrow [C_6H_5O_7H]^{2-} + OH^-$$

The bulky citrate anions are adsorbed preferentially on the polar Zn^{2+} (0001) plane, thereby suppressing the growth of ZnO perpendicular to this plane and enhancing growth along the nonpolar $\{10\bar{1}0\}$ planes [10]. When an intermediate amount of TSC is present in solution, the citrate ions enhance the lateral growth of each nanorod branch along

the six symmetry directions of $<10\bar{1}0>$ [14]. In this manner, neighboring ZnO nanorods growing along the same direction are merged together to form large hemispherical ZnO NSs. Therefore, TSC acts as a surfactant for the ZnO NSs and the shape evolution of ZnO NSs can be explained based on a surfactant-mediated growth mechanism. However, when the TSC concentration was increased to 3.9 mM, the ZnO NSs gradually disappeared, as shown in Fig. 2(i) and (j). This could be attributed to the increased pH of the solution as well as the complexation of Zn^{2+} ions with citrate anions, which inhibit the hydrolysis of Zn^{2+} ions [15].

Fig. 6 shows the PL spectra of the ZnO NSs at TSC concentrations of 0, 1.3 and 2.6 mM. The PL spectra of all samples exhibited two main emission peaks in the UV and visible ranges, which correspond to the band edge emission of ZnO and deep levels, respectively. The visible range emission of the ZnO NSs can be attributed to radiative recombination through point defects in the ZnO lattice, such as oxygen vacancies, zinc vacancies, oxygen interstitials, zinc interstitials, and anti-site defects [1,16,17]. The PL peak positions of UV emission for the ZnO NSs were all 381 nm. This suggests that the ZnO NSs were crystalline with a wurtzite structure, similar to the XRD results. The ZnO NSs grown with 1.3 mM TSC showed the highest deep level to band edge emission ratio, whereas that grown with 2.6 mM (ZnO hemisphere) showed the lowest ratio. This suggests

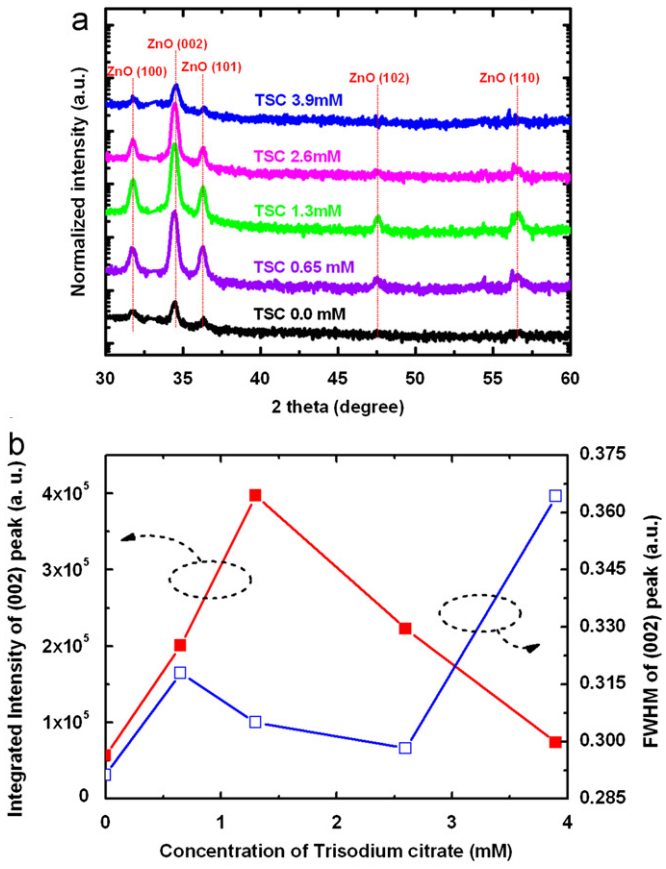

Fig. 4. (a) Normalized $\theta-2\theta$ XRD pattern of the ZnO NSs with various TSC concentration in the main solution. (b) Integrated intensity and FWHM of ZnO (002) peaks as a function of the TSC concentration in solution.

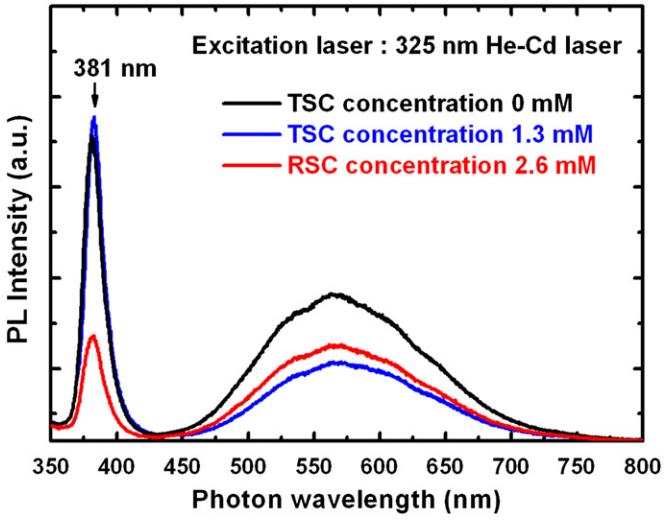

Fig. 6. Room temperature PL spectra of the ZnO NSs with various TSC concentrations in the main growth solution.

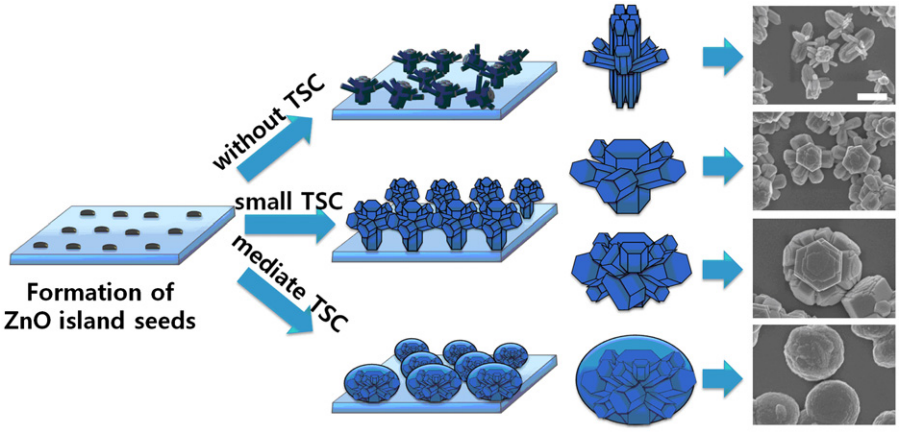

Fig. 5. Schematic diagram of the ZnO NSs formation with the variation of TSC concentration during the main growth solution. The scale bar in the SEM image is 500 nm.

that the crystalline quality of ZnO NSs was highest at a TSC molar content of 1.3 mM. This can be attributed to ZnO NSs being single crystals grown along the [0001] direction, as can be inferred from the well-faceted six-side surfaces with a hexagonal top facet of the ZnO NSs [12]. The decreased band edge emission of the ZnO hemispheres can be attributed to degradation of the crystalline quality of ZnO NSs as can be inferred from the XRD and PL results. Degradation of the crystalline quality of the ZnO hemispheres can be attributed to the suppression of ZnO growth along the preferred *c*-direction, resulting in defects and incorporation of impurities into the ZnO NSs. These results show that the morphology of ZnO NSs grown on Si substrates can be controlled by varying the concentration of additive TSC during hydrothermal growth.

4. Conclusions

In conclusion, we demonstrated a method for controlling the morphology of ZnO NSs for the fabrication of hemisphere structures. The ZnO NSs grown without addition of TSC displayed a flower-shaped morphology consisting of bundles of ZnO nanorods. With increasing TSC concentration to 2.6 mM, the ZnO nanorod bundles merged together to form large hexagonal crystals, and the morphology of ZnO NSs became hemispheric on Si substrate. Structural and optical measurements showed that ZnO NSs were crystalline ZnO with a wurtzite structure, and the crystalline quality differed according to the TSC concentration. The shape evolution mechanism of ZnO NSs could be explained by a surfactant-mediated growth model. Overall, these controllable ZnO NSs can be a promising multi-functional novel architecture for advanced photovoltaic and optoelectronic device applications.

Acknowledgment

This research was supported by Basic Science Research Program through the National Research Foundation of Korea (NRF) funded by the Ministry of Education, Science and Technology (2012R1A1A1001711) and by the IT R&D program of MKE/KEIT [10039151, the development of 200 mW level high power green (525 nm) LED for full color display].

References

[1] D.C. Look, Recent advances in ZnO materials and devices, Materials Science and Engineering: B Advanced 80 (2001) 383–387.
[2] S. Xu, Z.L. Wang, One-dimensional ZnO nanostructures: Solution growth and functional properties, Nano Research 4 (2011) 1013–1098.
[3] Y.W. Heo, D.P. Norton, L.C. Tien, Y. Kwon, B.S. Kang, F. Ren, S.J. Pearton, J.R. LaRoche, ZnO nanowire growth and devices, Materials Science and Engineering R 47 (2004) 147.
[4] Y.S. Lee, Y.I. Jung, B.Y. Noh, I.K. Park, Emission pattern control of GaN-based light-emitting diodes with ZnO nanostructures, Applied Physics Express 4 (2011) 112101.
[5] K.K. Kim, S.D. Lee, H. Kim, J.C. Park, S.N. Lee, Y. Park, S.J. Park, S.W. Kim, Enhanced light extraction efficiency of GaN-based light-emitting diodes with ZnO nanorod arrays grown using aqueous solution, Applied Physics Letters 94 (2009) 071118.
[6] K.S. Kim, S.M. Kim, H. Jeong, M.S. Jeong, G.Y. Jung, Enhancement of light extraction through the wave-guiding Effect of ZnO submicrorods in InGaN blue light-emitting diodes, Advanced Functional Materials 20 (2010) 1076–1082.
[7] K.S. Kim, H. Song, S.H. Nam, S.M. Kim, H. Jeong, W.B. Kim, G.Y. Jung, Fabrication of an efficient light scattering functionalized photoanode using periodically aligned ZnO hemisphere crystals for dye-sensitized solar cells, Advanced Materials 24 (2012) 792–798.
[8] T.Y. Wei, P.H. Yeh, S.Y. Lu, Z.L. Wang, Gigantic enhancement in sensitivity using Schottky contacted nanowire nanosensor, Journal of the American Chemical Society 31 (2009) 17690–17695.
[9] K.S. Kim, H. Jeong, M.S. Jeong, G.Y. Jung, Polymer-templated hydrothermal growth of vertically aligned single crystal ZnO nanorods & morphological transform using its structural polarity, Advanced Functional Materials 20 (2010) 3055–3063.
[10] S. Cho, J.W. Jang, S.H. Jung, B.R. Lee, E. Oh, K.H. Lee, Precursor effects of citric acid and citrates on ZnO crystal formation, Langmuir 25 (2009) 3825–3831.
[11] S. Cho, J.W. Jang, S.H. Jung, B.R. Lee, E. Oh, K.H. Lee, Formation of amorphous zinc citrate spheres and their conversion to crystalline ZnO nanostructures, Langmuir 27 (2011) 371–378.
[12] Y.I. Jung, B.Y. Noh, Y.S. Lee, S.H. Baek, J.H. Kim, I.K. Park, Visible emission from Ce-doped ZnO nanorods grown by hydrothermal method without a post thermal annealing process, Nanoscale Research Letters 7 (2012) 43.
[13] S.F. Wang, T.Y. Tseng, Y.R. Wang, C.Y. Wang, H.C. Lu, Effect of ZnO seed layers on the solution chemical growth of ZnO nanorod arrays, Ceramics International 35 (2009) 1255–1260.
[14] D. Andeen, J.H. Kim, F.F. Lange, G.K.L. Goh, S. Tripathy, Lateral epitaxial overgrowth of zno in water at 90 °C, Advanced Functional Materials 16 (2006) 799–804.
[15] L. Jia, W. Cai, H. Wang, H. Zeng, Polar-field-induced double-layer nanostructured ZnO and its strong violet photoluminescence, Crystal Growth & Design 8 (2008) 4367–4371.
[16] C.H. Ahn, Y.Y. Kim, D.C. Kim, S.K. Mohanta, H.K. Cho, A comparative analysis of deep level emission in ZnO layers deposited by various methods, Journal of Applied Physics 105 (2009) 013502.
[17] C. Wu, X. Qiao, L. Luo, L. Li, Synthesis of ZnO flowers and their photoluminescence properties, Materials Research Bulletin 43 (2009) 1883–1891.